

BOREHOLE GEOLOGY OF WELL FIALE 3, ASAL-FIALE GEOTHERMAL FIELD, DJIBOUTI

Ahmed, A.

Office Djiboutien de Développement de l'Energie Géothermique (ODDEG), route d'Arta PK 20, Djibouti

araksan_ahmed@yahoo.fr ; araksan.ahmed@oddeg.dj

Keywords: Geothermal, Asal-Fiale, Borehole, Alteration, Temperature reversal, Upflow.

ABSTRACT

The geothermal well Fiale-3 is located in the Asal-Fiale geothermal field, within the north-western part of the Fiale caldera. The well is directionally drilled to a total measured depth of 2660 m in a N224° direction. In the purpose of providing the stratigraphy, thermal conditions, and a detailed description of the geothermal reservoir characteristics of the well, binocular microscopy, thin sections petrography, XRD analysis and methylene blue analyses have been carried out. The lithostratigraphy of Fiale-3 is formed by four main stratigraphic units, which are the Asal series, the Afar stratoid series, the Dalha basalt series and Mabla rhyolite. Several alteration minerals have been observed with progressive depth and the occurrence of hydrothermal alteration minerals is related to their formation temperatures such as smectite ($\geq 40^{\circ}\text{C}$), quartz ($\geq 180^{\circ}\text{C}$), chlorite ($\geq 220^{\circ}\text{C}$), epidote ($\geq 230^{\circ}\text{C}$), and actinolite ($\geq 280^{\circ}\text{C}$). Further, Anhydrite has also been described from 700 m to deeper depth in the well. Anhydrite as sulphate mineral is a good indicator for fresh seawater infiltration. In total, five alteration zones can be classified. These are an unaltered zone (145 m), a smectite zone (145-550 m), a chlorite zone (550-792 m), an epidote zone (792-1283 m), and an epidote-actinolite zone (1283-2660 m). However, the observed alteration pattern does not present the thermal condition today. Measured temperatures within the well by downhole logging indicate a temperature reversal between 733 and 1700 m measured depth (MD) due to a large inflow of cold seawater through the NW-SE major faults of the rift. The absence of low-temperature minerals in the reversal zone may indicate that the geothermal system has not been equilibrated. This may indicate that the cooling is relatively young. Permeable zones are identified from circulation losses and temperature logs. The largest feed zone at 733 m (MD) is mainly controlled by the rift faults and led to the intrusion of cold seawater in the system. In general, the well shows a relative low permeability in the shallow and deep reservoir. The alteration and temperature models of Asal-Fiale geothermal field give no evidence for the existence of an upflow.

1. INTRODUCTION

The Republic of Djibouti is a territory of 23 000 km² located in East Africa. The country is situated in the south-eastern part of the Afar depression where three large-scale rift/ridge zones form an active triple-junction (Courtillot et al., 1987). The three zones are the intracontinental East African Rift, and the oceanic ridges of the Red Sea and the Gulf of Aden. The major rifting creates several disconnected rift segments that are stretching the crust and the lithosphere within the Afar rift (Tapponnier et al., 1990). The Asal-Ghoubbet rift is one of the emergent segments of the Aden Gulf ridge which spreads westward on land into the Afar depression (Manighetti et al., 1998). Different volcanic features associated with effusive events separated in time characterize the rift-in-rift area. One of them is the former central volcano Fiale that is characterized by a caldera structure. The Fiale caldera corresponds to the studied area in the present report (Figure 1). Still today, important seismic activity takes place in the area and fumaroles and hot springs are active.

Djibouti's geothermal exploration began in 1970. Geological, geochemical and geophysical studies have been undertaken in Djibouti to locate possible areas for geothermal development and exploration by the French Geological Survey (BRGM) in 1973. In 1975, the first two exploration wells were drilled in the southwestern part of the Asal-Ghoubbet rift. In 1987, four more deep wells have been drilled in the area (Aquater, 1989). Twenty years later, in 2008, a complete TEM and MT campaigns covering the Asal area carried out by the Iceland GeoSurvey (ÍSOR) for REI (Reykjavik Energy Invest) showed the existence of three separate geothermal fields, which are Gale le Koma and Asal NW in the south of Lake Asal, and Asal-Fiale, named after the Fiale caldera edifice (Dobre et al., 2007; Árnason et al., 2008).

The Asal-Fiale area was chosen in 2011 to drill three new deviated wells with large production diameter of 9 5/8" within the Fiale caldera in Asal Rift (AfDB, 2013). In the long term, the objective is to build a power plant able to produce 50 MW to support the increasing energy needs of the country. The drilling of the first well, Fiale 1 has been spudded on the 18th of July 2018. Three directional wells have been completed in the area with the following measured depths: 2745 m for Fiale 1, 2705 m for Fiale 2 and 2660 m for Fiale 3.

The objective of this study is to present the subsurface stratigraphy and thermal conditions of well Fiale 3, and the detailed description of the geothermal reservoir cut by the well. For this purpose, several analyses have been undertaken. It includes the analysis of cuttings under binocular microscope, the analysis of hydrothermal alteration minerals and their paragenesis. The classification and location of the alteration zones and the impact of the large intrusion of cold water have been studied with the help of XRD and petrographic analysis. Finally, the study of the temperature profile and the correlation of the lithostratigraphy and the alteration minerals between Fiale 3 and the surrounding wells will provide a better understanding of the geothermal system within the Fiale caldera.

2. GEOLOGY OF MANDA-INKIR FIELD

Located in the eastern part of the African continent, the Afar depression is the result of 30 Ma of separation of the continental plates of Arabia and Africa by the rise of a mantle plume in its lithosphere (Courtillot et al., 1999). The area is characterized by the occurrence of different active rifts. The Asal-Ghoubbet rift is one of the emergent segments of the Aden Gulf ridge which spreads

westward on land into the Afar depression (Manighetti et al., 1998). One of the youngest rifts within the Afar (0.9 Ma) (Varet, 1978), it is ~40 km long with only 15 km section and emerges in a NW-SE direction. It opens at 15 ± 2 mm/year along a direction of $N40^\circ \pm 5^\circ E$ (De Chabaliér and Avouac, 1994). It extends from the Gulf of Ghoubbet in the SE to Lake Asal in the NW. Moreover, the emerged part shows a dense network of fissures and sub-vertical normal faults with a strike of $N130^\circ \pm 10^\circ$ running from the northwest shore of the Lake Asal to the Ghoubbet basin, as shown in Figure 1 (Manighetti et al., 1998).

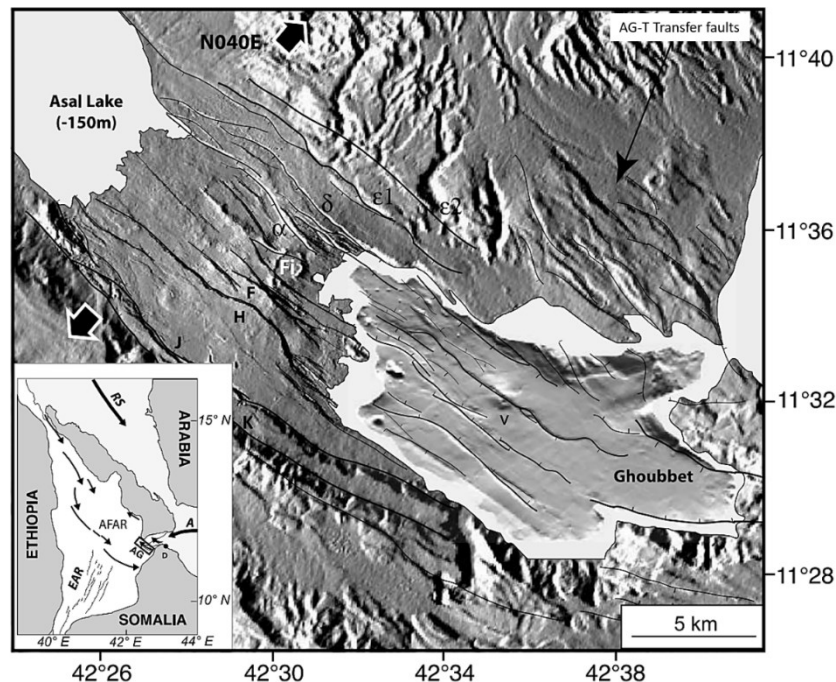


Figure 1: Topographic and tectonic map of Asal-Ghoubbet rift. Faults (α , δ , ϵ_1 and ϵ_2 , F, H, J, K) taken from Manighetti et al. (2001a, 2001b) and Audin et al. (2001). Fi stands for the Fiale caldera; v for the easternmost recent volcano in Ghoubbet and AG-T for Asal-Ghoubbet/Tadjoura transfer faults. The inset shows the general setting of the Afar depression, at junction between the East African Rift (EAR), the Red Sea Ridge (RS), and the Aden Ridge (A). D stands for Djibouti and arrows symbolize propagating, active rift segments. The Asal-Ghoubbet rift (AG) is indicated by a rectangle.

The rift-in-rift area has witnessed magmatic and tectonic activities over its whole evolution. Different phases of volcanic activity have alternated with phases of major faulting (Stein et al., 1991). The period between 853 ± 35 ka to 315 ± 53 ka allowed the formation of hyaloclastite (submarine pyroclastic rocks) during the time that the rift was below sea level (326 ± 15 ka) in the south part of the rift and magmatic activity remained effusive in the north (334 ± 43 ka and 315 ± 53 ka). During this first period, faulting has dismantled the lava formations (Manighetti et al., 1998). Between ~300 and 100 ka, the volcanic activity in the area was mainly animated by the central shield volcano Fiale. The inner floor and previous faults have been filled and covered by large basalt lava flows (Pinzuti, 2006). These lava flows may find their origin from a long-lived, deep magma chamber (Van Ngoc et al., 1981). Then, an “a-magmatic” period of 100 ka followed. This period is characterized by a high faulting activity that progressively cut the lava piles including the Fiale edifice. Only short phases of fissure eruptions interrupted this time, such as those responsible of the recent lava fields on either side of Fiale volcano (De Chabaliér and Avouac, 1994). The decreasing of the magmatic activity led the previous basalt lava flows that form the Fiale volcano to become gradually offset by normal faults. The structure of the modern rift started 40 to 30 ka ago and the northernmost faults (α to δ) are the youngest and presently the most active (see location in Figure 1) (Manighetti et al., 1998). From this tectonic period, the Fiale volcano collapsed and gave the ~1.5 km wide circular caldera known today. The rare magmatic activities were located within the inner floor along small volcanic edifices and fissure eruptions (Stein et al., 1991).

The most recent magmatic activity occurred in November 1978 (Abdallah et al., 1979). It corresponds to a major rifting episode associating two large earthquakes in the Ghoubbet (magnitude 5 and 5.3) and a one week-long basaltic fissure eruption at the northwestern tip of the volcanic chain, which gave birth to the Ardoukoba volcano (Demange et al., 1980). According to Ruegg (1979), this episode led to 2 m extension of the rift along the $N40^\circ E$ direction and a subsidence of 70 cm in the inner floor. Mechanical modeling of the deformation suggests that the rifting episode may be linked to the sudden opening of two 4 to 8 km long dikes at ~4–5 km depth in the rift’s inner floor, with the largest in the Ghoubbet (Tarantola et al., 1979, 1980).

In general, the Asal-Ghoubbet rift shows a major NW-SE trending extensional regime with numerous faults and fractures. Two major asymmetric faults represent a typical graben structure. Several faults trends have also been identified in the area, such as E-W faults resulting from rifting during Miocene in the Gulf of Aden and later in Tadjoura (Khodayar, 2008), N-S, and rare ENE. Based on the geological map of the rift in Figure 2, the more recent basaltic formations are located in the inner part with hyaloclastite and lacustrine deposits while the oldest basalts, of stratiform structure, are found in the outer part.

3. ASAL-FIALE GEOTHERMAL AREA

3.1 Geological review

The Fiale caldera is in the Asal-Ghoubbet rift axial graben between two boundary rift faults trending NW. It is a former volcano that has been active from ~300 to 80 ka (Manighetti et al., 1998). The inner part of the caldera is covered by young basaltic lava flows forming the so-called Lava Lake. The Fiale caldera is surrounded by a 1.5 km diameter rim that measures 20 to 30 m high. It is cut

by a dense network of approximately EW to NW striking open fissures and small normal faults. The Fiale caldera is almost entirely enclosed in that graben.

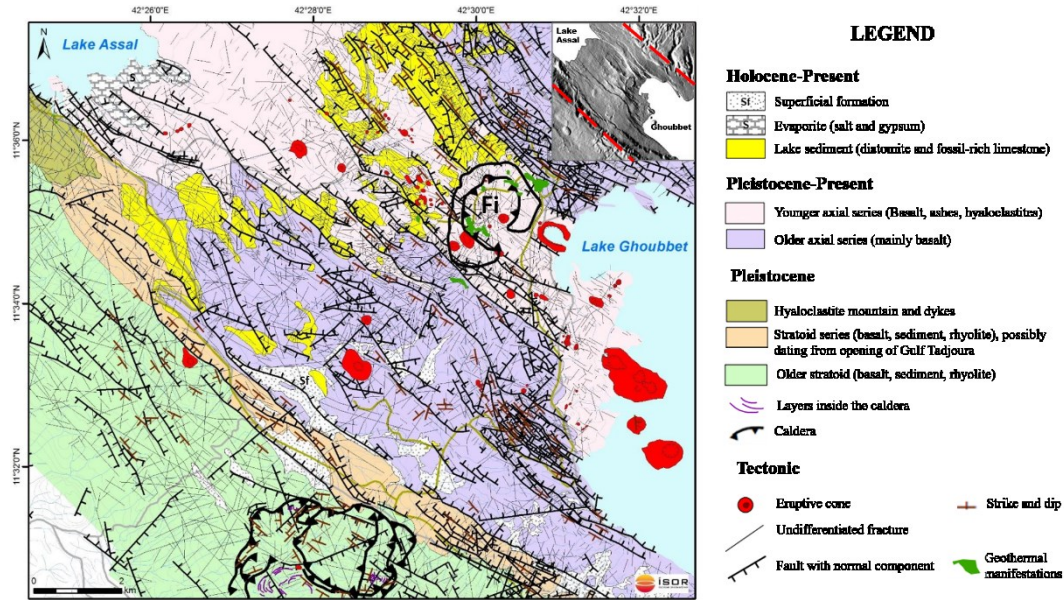


Figure 2: Geological map of the Asal-Ghoubbet rift between the gulf of Ghoubbet and Lake Assal, Fi: Fiale Caldera (modified from Khodayar, 2008). Main structures are NW-SE trending rift faults and NE-SW trending transform faults. The inset shows the boundaries of Asal-Ghoubbet rift.

Seismological studies carried out by Doubre et al. (2007) shed light on the transient magma-tectonic mechanisms that contribute to the rifting cycle. According to them, a main volcanic plumbing system is located at the center of the rift under the Fiale caldera. It corresponds to the focused zone of crustal production where a magma chamber is suspected. The whole caldera zone is found overlaying a 2 km wide central column of low seismic velocities that suggests the presence of hot intrusions above a deeper magma chamber at 5 to 6 km depth. Doubre et al. (2007) showed that the seismicity in the Fiale volcanic system zone occurs in successive periods (Figure 3). The latter (red in Fig. 3) are local seismic events observed at the basis of the faults. These events are caused by up and down vertical motions along the faults, especially along the Fiale ring faults in the east. The piston-like motions are likely related to inflation-deflation motions in the underlying magma reservoir and intrusions. Thereby, the probable presence of a magma chamber at shallow depth could represent the heat source of a geothermal system within the area.

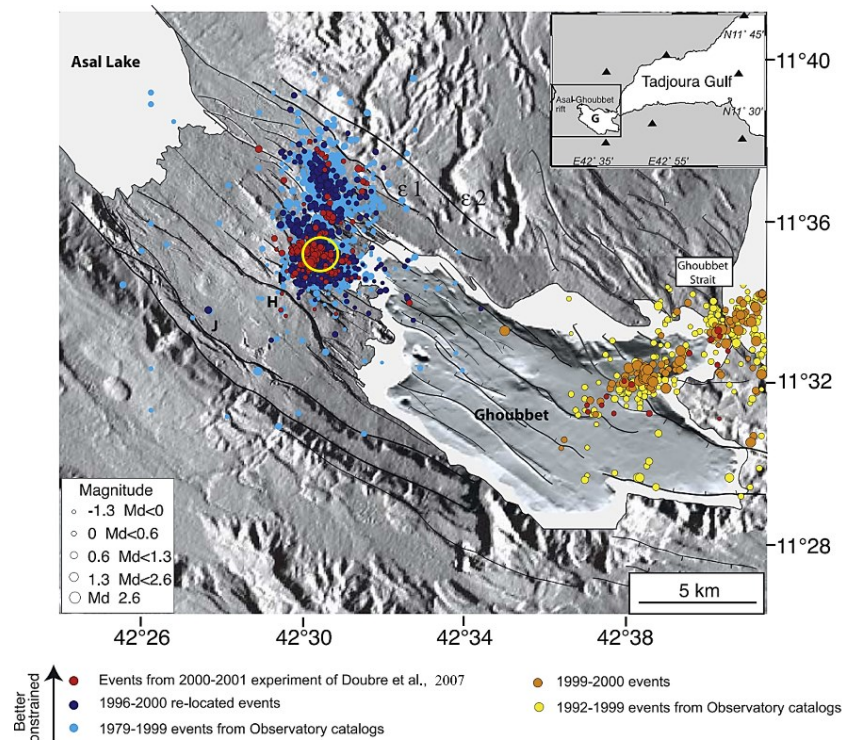


Figure 3: Distribution of seismic events between 1979 and 2001 in the whole Asal-Ghoubbet rift. Colors indicate data sets. Faults are in grey and the Fiale caldera area is the yellow circle. Inset shows permanent seismological stations (triangles) in the Ghoubbet (G) and Tadjoura Gulf regions (from Manighetti et al., 2001a, modified by Doubre et al., 2007).

3.2 Stratigraphy

In total, six deep wells have been drilled in the Asal-Ghoubbet rift between 1975 and 1987. The wells Asal 1, 2, 3, 4 and 6 are located in the south-western part of the rift and only Asal 5 is situated in the central part of the area, near the Fiale caldera (Aqater, 1989). Their location is given in the map in Figure 4.

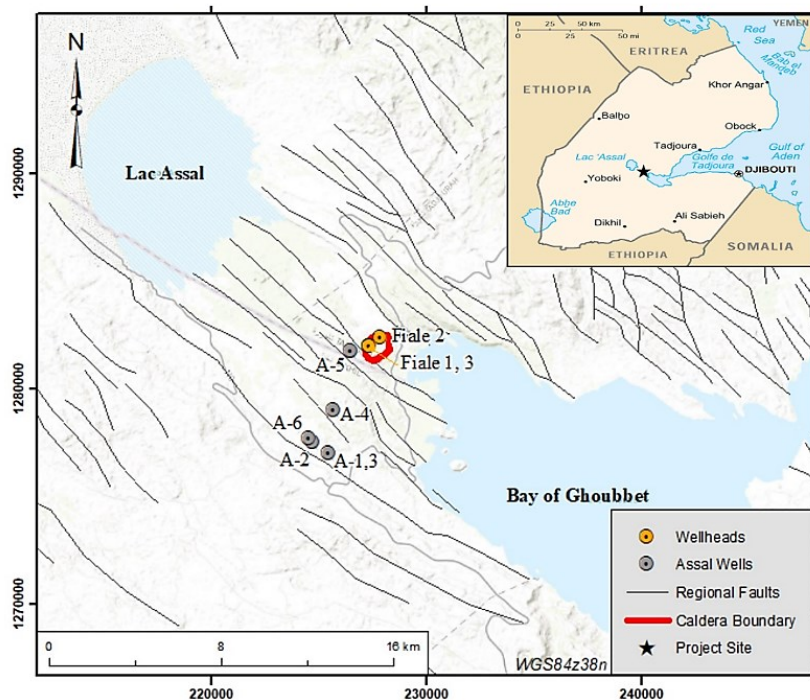


Figure 4: Location of Asal-Ghoubbet exploration wells (from Le Gall et al., 2015)

The main stratigraphic units encountered in the wells Asal 1 to 6 are given below from the top to the bottom and illustrated in the SSW-NNE cross section in Figure 5. The stratigraphy is based on ISERST (1985; 1986) and Barberi (1975), and summarized by Aqater (1989).

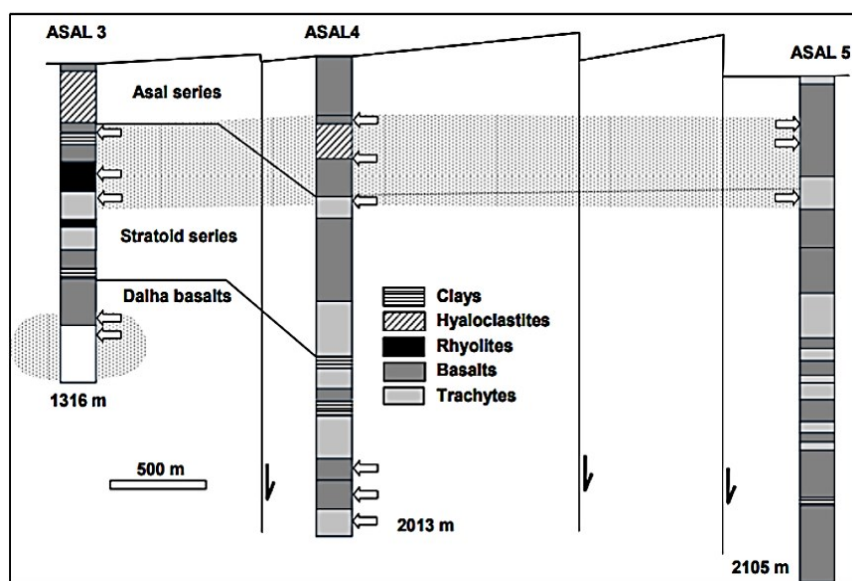


Figure 5: SSW-NNE cross section through the south-eastern part of the Asal-Ghoubbet Rift. The cross section shows the stratigraphy of wells A-3, A-4 and A-5 in Gale-Le-Koma and Fiale geothermal fields, the aquifers (arrows and grey areas) and the main faults in the explored area (taken from Aqater, 1989).

Asal series: This lithological unit comprises recent basaltic lava flows and hyaloclastites generated at the onset of the volcanism of the Asal Rift with a maximum age of 1.05 Ma. The unit can further be divided into the “Série des Marges Externes d’Asal”, outcropping on both sides of the rift and the “Série de la Zone Centrale d’Asal” as well as on a 3-4 km wide belt in the inner part of the Asal Rift.

Afar stratoid series: This unit overlies unconformably the the Dalha basalt series. The volcanism of the central Afar produced a sequence of basalt-dominated fissure flows that are associated with rhyolitic volcanic centers. The different products found in this unit are mainly basaltic, with intercalation of more evolved products such as trachytes and rhyolites. Lacustrine deposits are also found. The age ranges between 4 and 1 Ma.

Dalha basalts series: This lithological unit is formed by a sequence of basaltic lava flows intercalated with rhyolites, trachytes and detritic deposits. The reservoir zones were identified in this unit for the wells Asal 1, 3 and 6. The age of the Dalha basalt series ranges between 8.9 and 3.8 Ma.

3.3 Pre-drilling conceptual model

A conceptual model for Asal rift area has been proposed by ÍSOR for ODDEG in December 2017. The setting of this conceptual model is based on the previous and complete studies undertaken in the area, which is considered to have a viable geothermal potential. The data review included geological, geochemical, geophysical, hydrological and other available geoscientific data and interpretations related to the studied area.

In November 2017, geochemical analyses of samples from seven hot springs in Assal NW, at the border of the Asal Lake, were carried out by ÍSOR and ODDEG. The results show that the chemical composition is mainly from seawater of the Ghoubbet bay mixed with geothermal water on its way along the major NW-SE rift faults, and/or the sea water has been heated up due to high geothermal gradient. However, the high silica content in the spring water suggests a possible mixing with geothermal fluids from Fiale and/or Gale-Le-Koma reservoirs before flowing towards the Asal Lake.

Several geophysical studies have been undertaken in the area. According to Demange and Puvilland (1990), the residual Bouguer map shows that the low gravity anomalies correspond to the hyaloclastite volcanic formations found in the south- and north-western and south-eastern part of the rift. The high gravity values are mostly located in the inner part of the rift around the Lava Lake due to dense subaerial lava flows and/or dense intrusions at depth in the volcanic center. Then, the geophysical studies undertaken by Árnason et al. (1988, 2008) described a first high near-surface resistivity due to the fresh dry rocks above the groundwater table in the NW part of the rift. A low resistivity area is observed in the SE of a hydrological barrier perpendicular to the rift in a SW-NE direction (Figure 6). Then, the smectite layer (clay cap), characterized by low resistivity, is found at different depths in the Asal rift. A high resistivity layer below the cap rock might be formed by the precipitation of high temperature alteration minerals, such as chlorite and epidote, or by the decrease of porosity. Finally, a new low resistivity zone is detected below the high resistivity. Geothermal activity linked to hypersaline fluid can be the cause.

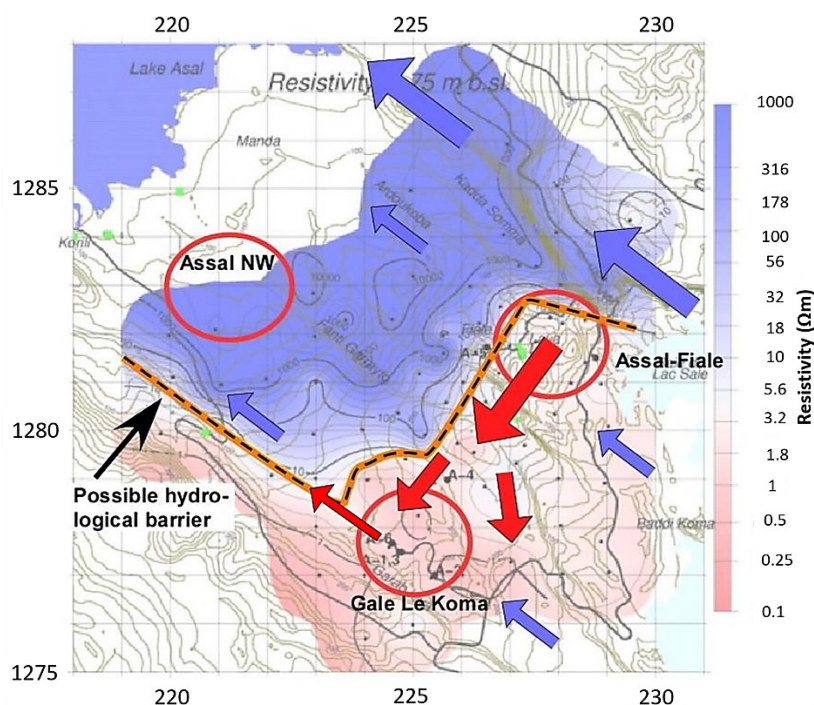


Figure 6: Hydrological barrier observed in the resistivity model (at 75 mbsl). Hot fluids coming under Lava Lake flows along leaky transform zones described by Khodayar (2008) to S and SW. The hydrological barrier is shown with orange/black dotted line. Red and blue arrows show proposed movements of hot and cold water along the major NW-SE fault zones at 100-200 m depth and 500-800 m depth. Taken from Árnason et al. (2008).

Árnason et al. (2008) proposed the first conceptual model of the Asal-Ghoubbet rift area based on the geophysical results (Figure 7). It consists of three distinct geothermal systems, which are Gale-Le-Koma in the SW, Assal-Fiale in the central part of the rift that includes the Fiale caldera and the Lava Lake, and Assal NW. The system under Lava Lake shows the presence of an important heat source more active than in Gale-Le-Koma and the formation of a convective geothermal system due to the heating of cold seawater by the hot magma intrusions at depth. The heated seawater becomes an upflow located under the Lava Lake and the precipitation of secondary minerals creates a hydrological boundary around the upflow zone. The seismic activity induced by the active rifting may open this barrier and let the geothermal fluid to escape along the fractures. Indeed, the well Asal 5, located in Fiale caldera area,

found a relatively high temperature (180°C) above 500 m. A lateral outflow of hot brine from the Lava Lake through the NNE-SSW trending faults (leaky transform zone) described by Khodayar (2008) may be the origin. However, the temperature drops to 80°C at 1000 m depth before rising to 350°C at 2100 m depth. The cooling could be explained by the inflow of cold seawater at 500 m depth throughout the major NW-SE faults in the Asal-Ghoubbet rift.

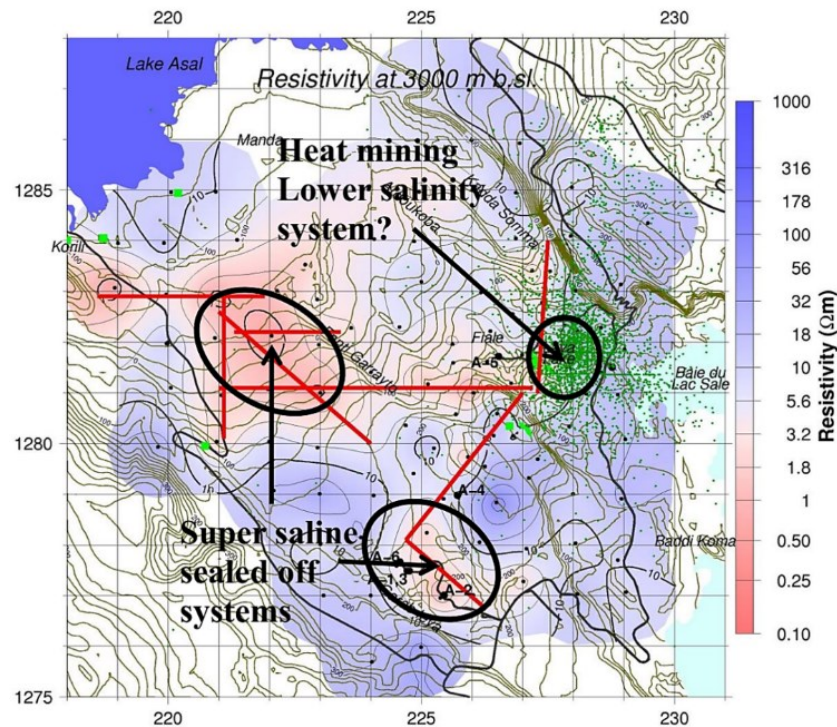


Figure 7: Conceptual model of geothermal activity in the Asal-Ghoubbet Rift (taken from Árnason et al., 2008). The figure shows resistivity at 3000 mbsl, inferred lineaments in low resistivity (red lines), seismicity (dark green dots) and geothermal surface manifestations (light green). Two main geothermal systems sealed off and super saline, and a more open lower salinity system under Lava Lake.

Therefore, the conceptual model by Árnason et al. (2008) summarized several characteristics/elements of the geothermal system in the Asal-Fiale zone. They are described as follows.

Origin of the geothermal fluid: Chemical and isotopic analyses suggest that the seawater from Ghoubbet basin is the origin of the geothermal fluids. However, the geothermal liquid presents a high salinity due to boiling within the system. Moreover, the cold seawater rich in sulphate component heats up and leads to the precipitation of anhydrite. Thus, anhydrite may fill the boundaries and decrease the permeability within the reservoir and between the surrounding geothermal systems. Indeed, these boundaries are shown in the resistivity model and are observed between Fiale/Lava Lake area and Lake Asal in an NNE-SSW trend. These hydrological boundaries limit the flow at shallow depths between Asal-Fiale/Gale-Le-Koma systems and Lake Asal (Árnason et al., 2008).

Size of the geothermal system: The difference of salinity and the possible presence of a hydrological barrier suggest a limited hydrological connection between Gale-Le-Koma and Asal-Fiale geothermal systems, on one part, and Asal NW on the other.

Boundary conditions: Well Asal 5 in the Fiale caldera area does not show clay beds such as found in Gale-Le-Koma between 400 m and 600 m depth. Thus, hydrothermal alteration minerals (i.e. smectite) may control the shallow boundaries. The flow of water in the system may be limited by the active major faults of NW-SE direction. The vertical barriers around Asal-Fiale and Gale-Le-Koma are probably sealed by anhydrite and other alteration minerals. Finally, the lower boundaries are controlled by the hot brittle/ductile intrusions at 4-5 km depth as seen in Figure 8 (Árnason et al., 2008).

Heat source: Seismic studies show that there is no shallowing lying magma chamber under Fiale/Lava Lake. Therefore, the heat source in Asal-Fiale system might be a combination of high thermal gradient due to crustal thinning and presence of hot intrusions at depth. Magma bodies may be found at greater depth than 5-6 km. In that case, the ductile boundaries, pointed out previously, may prevent the escape of magmatic fluids from greater depth.

3.4 Drilling of the well Fiale 3

The well Fiale 3 is located in the north-western part of the Fiale Caldera in the Lava Lake, on the well pad number 2. The geographical coordinates of the well are projected in UTM Zone 38N using WGS 84 datum. They are 1281976N and 227346.4E at an elevation of 109 m above sea level (masl). It is a directional well drilled to a measured depth of 2660 m in a N224° direction and a maximum of 30° inclination. All depth values are referenced to the rig floor that is 7.8 m above the surface. The well was drilled from 6th January to 23th February 2019.

The Icelandic Drilling Company was in charge of the drilling of well Fiale 3 for Electricité de Djibouti (EDD), using the drill rig Týr. Drill cutting analysis and geothermal consultancy services were conducted by ÍSOR (Iceland GeoSurvey). The drilling was carried out in four phases (Figure 9).

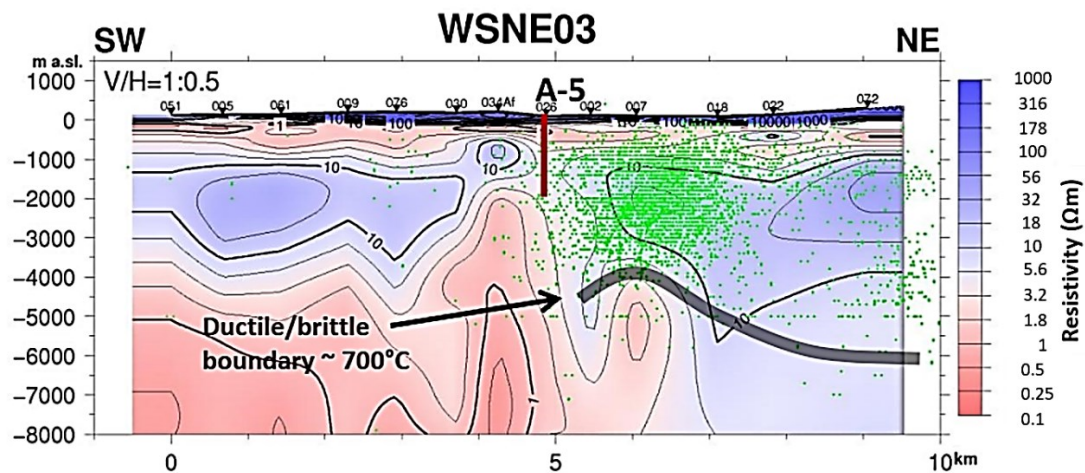


Figure 8: Resistivity cross section across the Asal-Ghoubbet Rift and location of earthquakes projected on the section. Estimated brittle/ductile boundary is indicated by the grey line below the deepest earthquakes. The maximum hypocenter depth rises below the Lava Lake, indicating a possible heat source below. From Árnason et al. (2008).

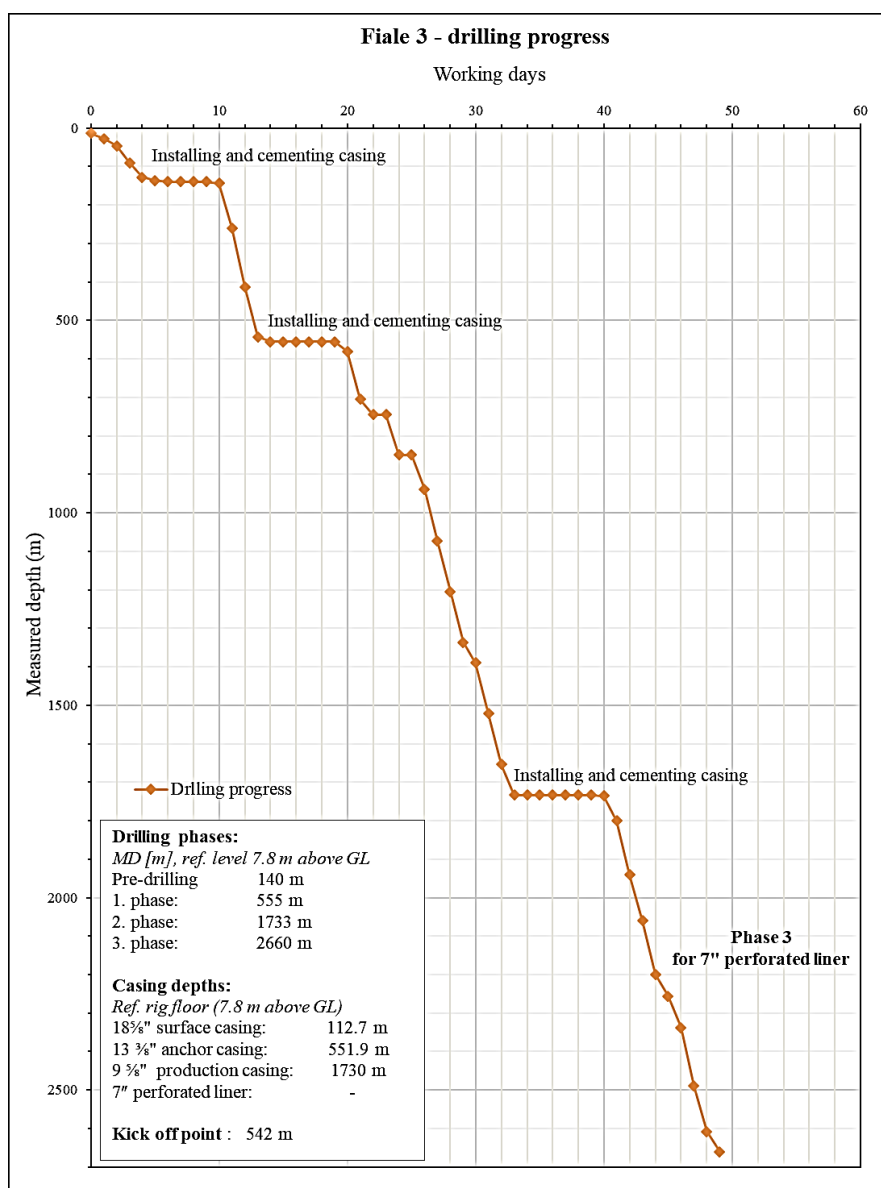


Figure 9: Scheme of drilling of well Fiale 3.

Pre-drilling phase reached a casing depth of 140 m on 12th of January. The 18 3/4" surface casing was set at a depth of 112.7 m. Drilling of phase 1 was launched on 16th of January and reached a depth of 555 m on 20th of January. The kick off point (KOP) of the well was set at 542 m. The maximal inclination is 30° with an azimuth of 224°. Then, the 13 3/8" anchor casing was set at 551.9 m depth. Phase 2 started on 25th of January. A depth of 1733 m was reached on 7th of February. The 9 5/8" production casing was run downhole to 1730 m. Finally, drilling of phase 3 (7" slotted liner) started on 15th of February and reached a measured depth of 2660 m on 23rd of February 2019.

4. ANALYTICAL METHODS

This study is based on the rock cutting samples collected during the drilling of Fiale 3. The drill cuttings were sampled every 5 m intervals from the surface to 555 m (MD) and every 3 m between 555 m and 2660 m (MD). Preliminary analysis using binocular microscope was done at the rig site carried out by the rig geologist. The first information obtained are the lithological composition and alteration mineralogy based on the physical or chemical properties of the minerals. These properties are the color, crystal habit, texture, grain size, structure, effervescence in contact with diluted HCl and general composition of the rock. The presence of vein fillings, fragments of intrusive rocks, oxidation and alteration intensity were also noted. For further analysis in ÍSOR laboratory, 48 samples were analyzed in more detail to refine the lithology and alteration. The samples correspond approximatively to every 50 m intervals. For binocular analysis, an Olympus SX16 microscope was used.

The second analysis was the petrographic microscope analysis. In total, 11 thin sections were studied with the aid of Leica DM 2700 P, petrographic microscope at the ÍSOR laboratory. The epoxy used for thin section was stained blued in order to make the porosity easier visible. The objective was to identify and confirm the rock type previously obtained during binocular analysis, and to determine the hydrothermal alteration minerals and their paragenetic sequences as observed in veins and vesicle fillings. In this study, the main goal was to focus on the effect of the temperature reversal from 700 m to 1700 m (MWD).

Methylene blue absorption test is a reliable and simple method to obtain information on the presence of clay minerals in soils and rock cuttings in this case. Helpful in the early stages of drilling, the amount of methylene blue adsorbed by the rock sample indicate

the presence of swelling clay minerals (Verhoef, 1992). The total absorbed amount allows calculate the methylene blue value, and cation exchange capacity (CEC) of the rock. This simple and quick method has been used on the rig site by analyzing the volume of smectite in samples approximatively every 20 m. The results, summarized in Appendix I, helped to delineate the interval depth of smectite zone by combining with XRD analysis.

The X-ray diffractometer (XRD) is an instrumental technique used to identify fine-grained clays and other crystalline materials that are not easily identified with other techniques. It is a basic technique for clay mineral analysis (Moore and Reynolds, 1989). Eight rock cuttings samples were chosen for clay analysis from depths of interest.

5. RESULTS

5.1 Lithostratigraphy

The lithology and alteration history of the well Fiale 3 is the result of two methods, based on the binocular and petrographic microscopy techniques. The lithological log, shown in Figure 10, is dominantly based on the rock cuttings analysis undertaken on the rig site during the drilling of the well. The thin sections analysis helped to verify the rock type and to analyze the alteration minerals assemblage in the depths of interest.

The lithological formations encountered are dominantly formed by the alternation of basaltic lavas and intermediates rocks. Acidic rocks are identified at the lowermost part of Fiale 3. The formations were divided into four main stratigraphic units which are the Asal series (0-440 m), the Afar stratoid series (440-1022 m), the Dalha basalt series (1022-2240 m) and the Mabila rhyolite (2240-2660 m). The description of these rock units is presented below.

5.2 Hydrothermal alterations

5.2.1 Alteration of primary minerals

Hydrothermal alteration is the interaction of the host rocks with the hot water and steam that leads to the dissolution of primary minerals and the deposition of secondary minerals by replacement and precipitation (Henley and Ellis, 1983). Several factors influence the degree of alteration such as the permeability, the temperature, the rock type, the hydrothermal fluid composition, the duration of the water-rock interaction, the number of superimposed hydrothermal regime, and the hydrological parameters (Kristmannsdóttir, 1976). Therefore, the changes in the hydrothermal environment let to the secondary minerals to precipitate partly in open spaces such as cavities, vesicles and fractures in the rocks. The primary minerals in the groundmass are also replaced by secondary minerals.

The primary minerals in well Fiale 3 include mainly feldspars (plagioclase and K-feldspar), pyroxene, opaque minerals, very rare quartz, olivine and glass, whereas olivine and glass show high degree of alteration. In fact, the primary minerals formed at high temperature present a weak resistance to hydrothermal alteration (Stefánsson et al., 2001). The description of primary minerals alteration is detailed below and summarized in the Table 1.

Volcanic glass is the most unstable phase and the first to be altered. Glass in well Fiale 3 has been very rare to examine. It alters to clays, calcite, and quartz.

Olivine is a magnesium-iron silicate. This primary mineral crystallizes rapidly during the cooling of the magma. It is also the first to alter. In this case, olivine was rarely observed at 300 m depth and has been altered into oxides at the shallow part. It can also be replaced by pyrite, chlorite and other green clays with the presence of the magnesium component.

Pyroxene is the most significant and abundant group forming ferromagnesian silicates and represent one of the main primary minerals observed in Fiale 3. Pyroxenes appear as small phenocrysts in the groundmass and individual large euhedral phenocrysts of clinopyroxene. They show different rate of alteration throughout the petrographic analysis. At 2050 m and 2351 m, the large crystals present a lower alteration degree. They alter into clays but also in epidote and actinolite.

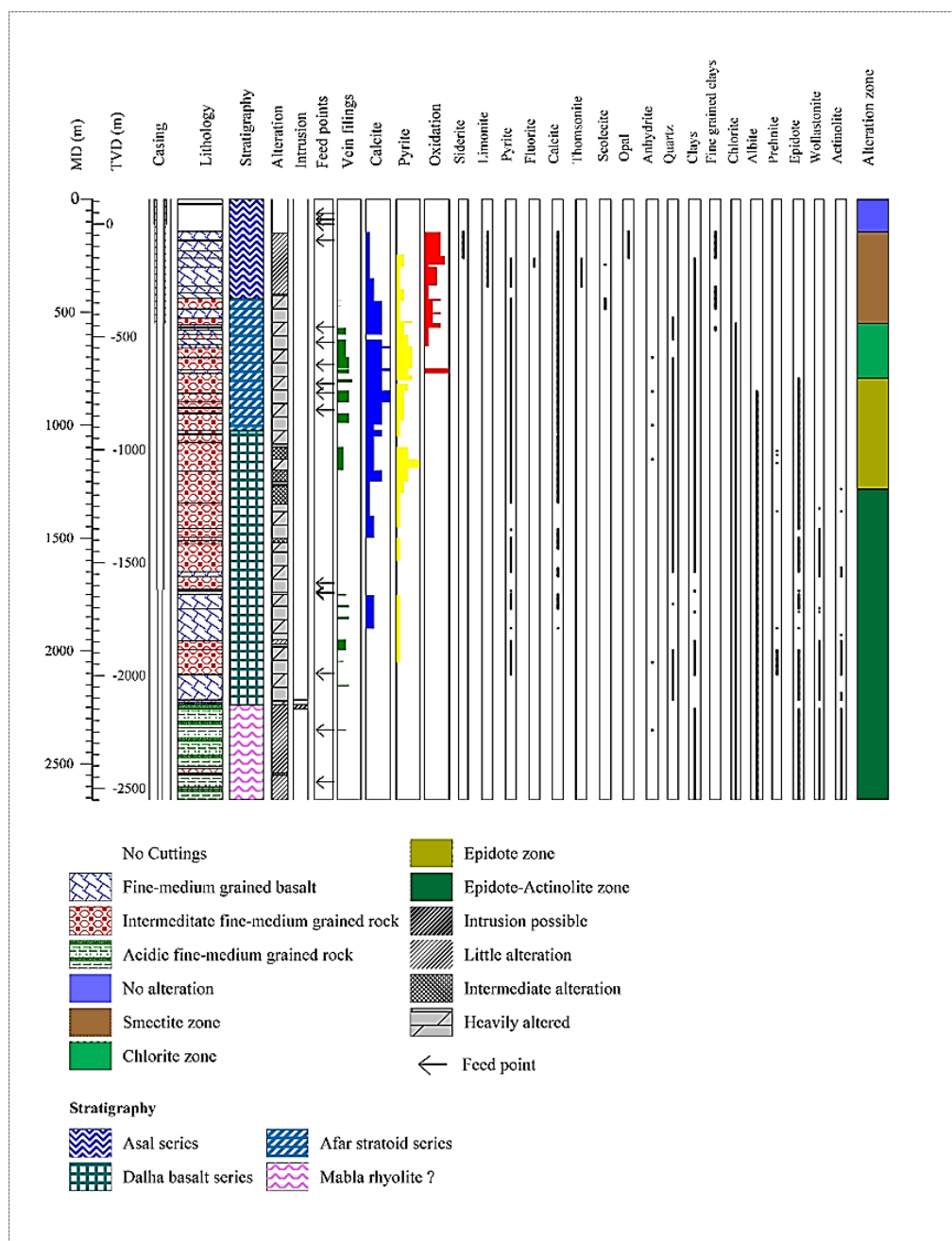


Figure 10: Distribution of lithology and alteration minerals in Fiale 3.

Feldspars minerals are the most abundant in igneous rocks. Plagioclases have been found in the different formations of the well described previously. They appear colorless to white, flat, columnar or granular and present a parallel cleavage under binocular microscope. They are identified by their low relief and polysynthetic twinning under petrographic microscope. They occur as fine in the groundmass but also large in rocks exhibiting porphyritic textures. Fresh in the upper part, feldspar present fluid inclusions along their twinning. They are fractured, and clays are formed along the fractures. They alter into albite, epidote, calcite, secondary quartz.

Potassium feldspars are also observed in the evolved formations, such as intermediate and acidic rocks. Sanidine is very common and is readily identified by its low relief, weak birefringence and simple twinning. Less observed, microcline is found at 1001 m, 1302 m, and 1449 m. They stay relatively fresh but can give the same alteration products.

Opaque minerals occur all along the well in different amounts. Magnetite is isotropic and appears opaque under petrographic microscope. It is present in a major amount in the deepest formations.

Quartz occur regularly in the rock. However, most of the quartz seems to be formed during secondary processes.

Depth (m)	Rock	Primary minerals	Alteration degree	Alteration minerals
-----------	------	------------------	-------------------	---------------------

300	Basalt	Volcanic glass	XXX	Clays, Cal
		Olivine	XXX	Clays, Cal
		Pyroxene	X	Clays
		Feldspars		
		Opaque minerals	XX	Py, Lm
450	Intermediate rock	Volcanic glass	XXX	Clays, Cal
		Olivine	XXX	Clays, Cal
		Pyroxene	X	Clays, Cal
		Feldspars	X	Clays, Cal
		Opaque minerals	XX	Py, Lm
700	Intermediate rock	Volcanic glass	XXX	Clays, Cal
		Olivine	XXX	Clays, Cal
		Pyroxene	X	Cal, Chl
		Feldspars	XX	Cal, Qz, Chl
		Opaque minerals	XX	Py
851	Intermediate rock	Volcanic glass	XXX	Clays, Cal
		Olivine	XXX	Clays, Cal
		Pyroxene	X	Cal, Chl
		Feldspars	XXX	Clays, Cal, Qz, Chl, Ab, Ep
		Opaque minerals	XX	Py
1001	Intermediate rock	Volcanic glass	XXX	Clays, Cal
		Olivine	XXX	Clays, Cal
		Pyroxene	XX	Chl, Ep
		Feldspars	XX	Cal, Qz, Chl, Ab, Ep
		Opaque minerals	X	Py
1151	Intermediate rock	Volcanic glass	XXX	Clays, Cal
		Olivine	XXX	Clays, Cal
		Pyroxene	XX	Chl, Ep
		Feldspars	XX	Cal, Qz, Chl, Ab, Ep
		Opaque minerals	X	Py
1302	Intermediate rock	Volcanic glass	XXX	Clays, Cal
		Olivine	XXX	Clays, Cal
		Pyroxene	XX	Chl, Ep, Act
		Feldspars	XXX	Cal, Qz, Chl, Ab, Ep, Act
		Opaque minerals	X	Py

1449	Intermediate rock	Volcanic glass	XXX	Clays, Cal
		Olivine	XXX	Clays, Cal
		Pyroxene	XX	Chl, Ep, Act
		Feldspars	XX	Cal, Qz, Chl, Ab, Ep, Act, Wo
		Opaque minerals	X	Py
1900	Basalt	Volcanic glass	XXX	Clays, Cal
		Olivine	XXX	Clays, Cal
		Pyroxene	XX	Chl, Ep, Act
		Feldspars	XX	Cal, Qz, Chl, Ab, Ep, Act, Wo
		Opaque minerals		
2050	Intermediate rock	Volcanic glass	XXX	Clays, Cal
		Olivine	XXX	Clays, Cal
		Pyroxene	XX	Chl, Ep, Act
		Feldspars	XX	Qz, Chl, Ab, Ep, Act, Wo
		Opaque minerals		
2351	Acidic rock	Pyroxene	XX	Chl, Ep, Act
		Feldspars	XXX	Qz, Chl, Ab, Ep, Act, Wo
Keys: Cal: Calcite; Lm: Limonite; Py: Pyrite; Qz: Quartz; Chl: Chlorite; Ab: Albite; Ep: Epidote; Act: Actinolite; Wo: Wollastonite; Alteration degree: X: slightly altered; XX: medium altered; XXX: highly altered.				

Table 1: Alteration of primary minerals based on petrographic and X-ray diffraction analyses.

5.2.2 Distribution of alteration minerals

The distribution and abundance of the hydrothermal minerals were obtained from the petrographic and binocular microscopy observations, and XRD analysis. The main hydrothermal minerals in Fiale 3 are actinolite, albite, anhydrite, calcite, different types of clays, epidote, pyrite, and quartz. In addition, minor amounts of fluorite, prehnite, and zeolites such as scolecite and thomsonite are found. Their distribution by increasing of temperature is summarized below.

Oxides are mainly iron oxides and form in the surface or near surface environments where oxygen-rich fluids interact with the rock. Oxidation is observed from the top of the well to 550 m depth. Limonite occurs. It forms by the oxidation of ferrous minerals such as magnetite observed in the ground mass.

Pyrite crystals are very common in the well from the shallower depth to 1500 m depth. It becomes very rare between 1500 m and 1650 m. It occurs again before appearing in trace between 1800 m to the bottom. It forms euhedral cubic crystals with brassy yellow metallic color. In thin section, it is opaque and with a granular form only observed by reflected light. It appears as a replacement of opaque minerals disseminated in rock groundmass and infillings in open spaces such as fissures, veins and vesicles.

Fluorite is very rare. It occurs at two intervals, 260 to 300 m and 440 to 485 m depth. It has been observed only during the cutting analysis. It forms cubes, octahedrons or spheres. It is colorless, greenish or pale violet.

Calcite is the most abundant alteration mineral observed continuously from 180 m depth to the bottom of the well. However, its amount varies, more present in the upper part and less in the deeper part. It is generally white with a vitreous luster and appears granular. It effervesces in dilute hydrochloric acid. In thin section, calcite is recognized by its high birefringence, three perfect cleavages and twinkling relief upon rotation of the microscope stage. In general, it appears as replacement of plagioclases. It can also be found as deposit in vesicles and fractures, forming sequences with clays, epidote, quartz and anhydrite.

Zeolites occur rarely in Fiale 3. They belong to a group of authigenic minerals, which precipitate extensively from alkaline hot water in geothermal systems. Their occurrence depends mostly on the temperature (Bird et al., 1984, Weisenberger and Selbekk, 2009, Spürigin et al., 2019). Most of them are low-temperature minerals characterized by deposition temperatures between 40 and 120 °C. Zeolite minerals occur only rarely and were only identified during cuttings analysis. Thomsonite forms white dense masses of radiating crystals with spherical clusters filling vesicles. It was found in low amount between 260 m and 385 m. The second zeolite observed is scolecite. It forms colorless radial crystals and is noted at 260-300 m and 440-485 m.

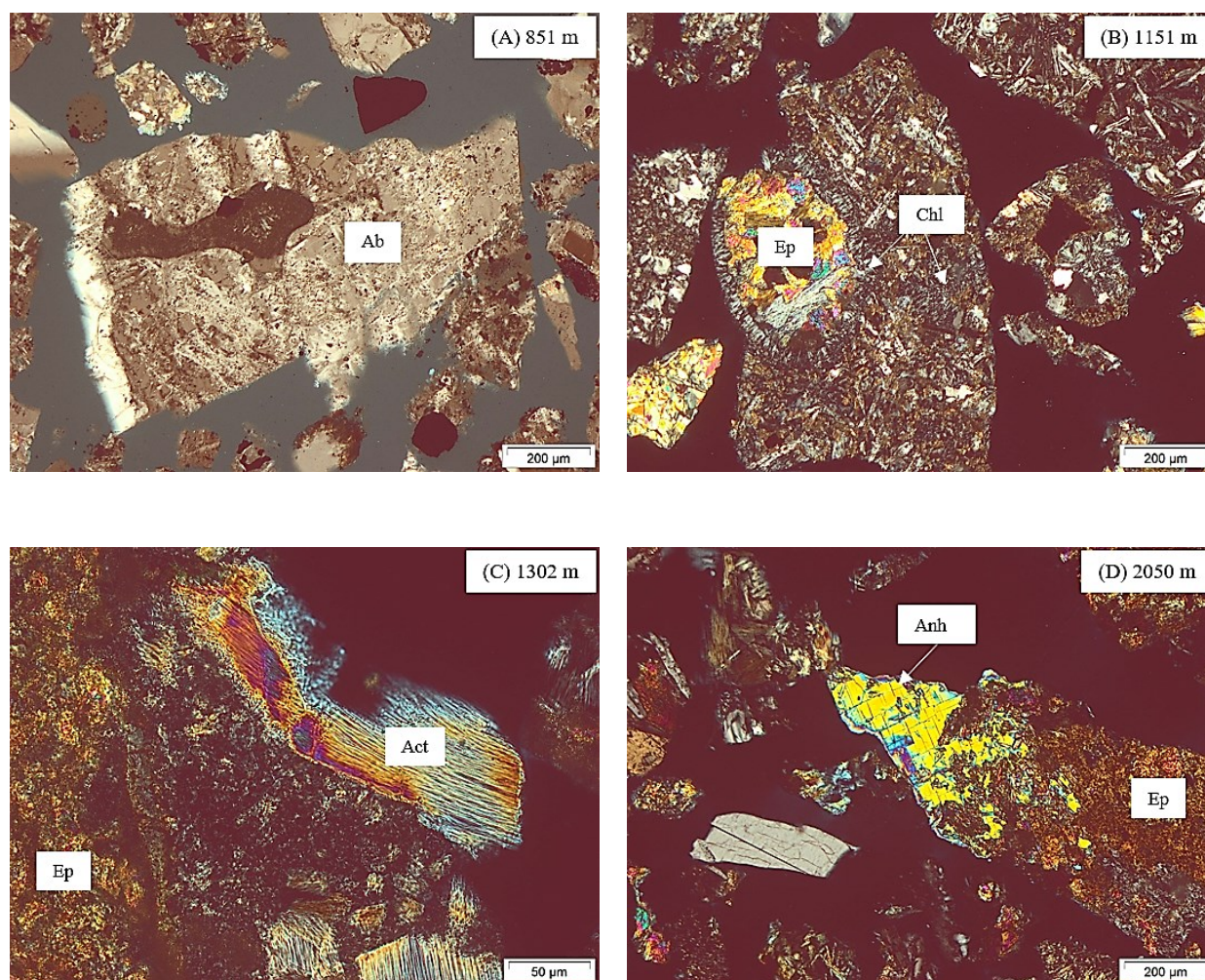


Figure 11: Thin sections, crossed Nicols (XPL): (A) Ab: Albite; (B) Vesicle filled by chlorite (Chl) and epidote (Ep); (C) Act: Actinolite; (D) Assemblage of epidote (Ep) of anhydrite (Anh)

Anhydrite (CaSO_4) forms when sulphate-rich seawater mixes with hot calcium-rich hydrothermal fluid or it becomes insoluble when seawater is heated to high temperatures above 150°C (Marks et al., 2010). In well Fiale 3, anhydrite occurs between 700 m and 1151 m under petrographic microscope. It appears again at 2050 m and 2351 m. In thin section, it is colorless with a moderate positive relief in PPL and has a high birefringence in third order in XPL (Figure 11). It occurs in aggregates of anhedral to blocky crystals at 1151 m and with epidote at 2050 m. It can also form euhedral elongated fibers. Its presence is explained by the large intrusion of cold seawater in the rift throughout the faults in direction to the Lake Asal.

Quartz is colorless to white and occurs in euhedral to subhedral crystals. It is identified under binocular microscope at 525 m depth. In thin section, it is found as infillings rare veins, fissures and vesicles. It can also appear as an aggregate of crystals. It is associated with other minerals such as calcite, pyrite, and epidote. Quartz forms at around 180°C .

Clays are common and abundant alteration products in hydrothermal system. They are hydrous phyllosilicates and are found in both high- and low-temperature fields (Kristmannsdóttir and Tómasson, 1978). According to Ahmed (2008), the composition, morphology and structure of clays depend on different factors, such as host rocks, temperature, fluid composition. The occurrence of clay minerals can help to interpret the thermal history of a geothermal system (Reyes, 2000). Clays were identified by XRD, petrography and binocular analysis.

- *Smectite* is a low-temperature clay mineral occurring as replacement of primary minerals. XRD analysis and methylene blue test results show the presence of smectite between 145 and 550 m (MD). It corresponds to the clay cap rock.
- *Mixed layer clay (MLC)* has been found with chlorite at 550 m by XRD.
- *Chlorite* starts to form at an equilibrium temperature of 220°C . It was identified at 700 m with MLC by using XRD analysis. Its occurrence is observed to the bottom of the well.

Albite is the alteration product of primary K-feldspar and plagioclase phenocrysts replacement. With the increase of temperature, the process of albitization leads to the disappearance of the twinning of the feldspars and give a cloudy appearance (Figure 11). Albite is noted from 851 m to the bottom. It forms at temperatures above 180°C .

Epidote occurs first at 792 m depth and stays abundant to the bottom of the well. It is yellowish-green color with a strong relief in PPL. It has a high birefringence with a yellow to green color in XPL. First crystals are anhedral and form fine-grained aggregates and in deeper zones, they appear idiomorphic, tabular, radiated or fibrous. Epidote is found as replacement of primary feldspar and

pyroxene but also filling the veins and vesicles in association with, albite, quartz, chlorite, actinolite, calcite, and pyrite (see Figure 11).

Wollastonite occurs an aggregate of elongated fine radiating crystals with a typical white to grey color. It is observed first at 1371 m. In thin section, it is colorless to white with a low interference color of first order grey. It is associated with epidote and anhydrite at 2050 m. Wollastonite indicates temperatures above 270°C.

Actinolite belongs to the amphibole group and is formed as a replacement of primary minerals such as pyroxene and plagioclase. It appears green to pale-green radiating fibers and massive to granular aggregates in the groundmass and individual crystals. It was first observed at 1283 m under binocular microscope and at 1302 m in thin section (Figure 11). It is present in the rest of the well. It occurs in association with epidote, albite and chlorite, and indicates high temperatures above 280°C.

5.2.3 Alteration mineral zones

In Fiale 3, five alteration mineral zones have been identified. Each zone is marked by the first occurrence of a higher temperature alteration mineral, which is indicative of increasing temperatures. Based on the results of binocular, petrographic and XRD analysis, the alteration zones are described as follows, and summarized in Figure 10. The alteration zones indicate a prograde alteration system.

Unaltered zone (<145 m): The lithology in this interval consists of fresh basaltic lava flows slightly oxidized. This zone is also characterized by total losses of circulation.

Smectite zone (145-550 m): This zone corresponds to the clay cap characterized by the presence of smectite clay. The mineral has been identified with XRD and methylene blue test. However, calcium sulfate mineral has been found at 450 and 550 m. It could be anhydrite mineral, formed as a result of fresh seawater infiltration.

Chlorite zone (550-792 m): This interval is defined by the occurrence of chlorite mainly unstable. At 700 m, a small peak of mixed layer clay is detected.

Epidote zone (792-1283 m): This zone is characterized by the first appearance of the epidote at 792 m. Chlorite is also very common. Other alteration minerals include albite, quartz, and anhydrite.

Epidote-Actinolite zone (1283-2660 m): This zone is identified by the occurrence of actinolite at 1283 m. High-temperature alteration minerals are also common in this interval such as epidote, chlorite, wollastonite, albite, and quartz. Anhydrite is also observed in thin sections and at 1151 m in XRD analysis.

5.2.4 Hydrothermal alteration mineral deposition sequence

According to Brown (1978), deposition of alteration minerals in open spaces such as vesicles, veins, vugs and fractures depends on various factors, which are porosity, permeability, temperature, fluid composition and the duration of the interactions. The study of the sequences of mineral deposition informs on the process involved, the time, and the temperature changes within the studied well.

In a first time, the observation of thin sections allows to determine and/or to confirm the different alteration minerals observed in the well Fiale 3. Their occurrence is summarized in the Table 2.

Depth m (MD*)	Alteration minerals									
	Cal	Py	Anh	Qz	MLC	Chl	Ab	Ep	Wo	Act
300	X	X								
450	X	X	X							
700	X	X	X	X	X	X	X			
851	X	X	X	X		X	X	X		
1001	X	X	X	X		X	X	X		
1151	X		X	X		X	X	X		
1302				X		X	X	X		X
1449	X	X		X		X	X	X		X
1900	X	X		X		X	X	X	X	X
2050			X	X		X	X	X	X	X
2351	X		X	X		X	X	X	X	X

Abbreviations: Act: Actinolite; Ab: Albite; Anh: Anhydrite; Cal: Calcite; MLC: Mixed Layer Clay; Chl: Chlorite; Ep: Epidote; Py: Pyrite; Qz: Quartz; Wo: Wollastonite; MD*: Measured Depth.

Table 2: Occurrence of alteration minerals based on binocular, petrographic and XRD analysis.

In open spaces, the determination of paragenetic sequences is based on the principle of mineralization order. The mineral on the edges of fractures, veins or vesicles is older than the next layer. Then, as explained in 5.2.1, primary minerals are altered and replaced by secondary minerals. Therefore, in mineral replacement analysis, the replacing mineral is younger than the former primary mineral. Cross-cutting relationships in crystals also help to establish the paragenetic sequence. Overprinting features and textural form in

minerals give information on the time and/or the temperature regime within the reservoir. Indeed, when a lower temperature mineral overprints a high temperature mineral, it indicates a change in the thermal regime, in this case a cooling of the system.

After the analysis of alteration minerals under petrographic microscope, their deposition sequences are detailed in the Table 3. The observation shows that most of the hydrothermal minerals have been formed by replacement and assemblage. Vesicles and fractures were more difficult to determine, due to their probable crushing during the drilling and the consequently small size of the cuttings. The paragenetic sequences expose two different thermal regimes. In fact, a prograde regime is shown when higher temperature minerals overprint or are formed after low-temperature minerals. However, in the case of Fiale 3, it is also shown that lower temperature minerals (e.g. calcite, quartz, anhydrite) are deposited after high-temperature ones such as actinolite, wollastonite or epidote. The deposition sequences suggest that the reservoir has experienced a cooling.

Depth m (MD)	Lithology	Mode of occurrence	Sequence from old to young
300	Basalt	Vesicle	Fine-grained clay - Calcite
450	Intermediate rock	Fracture/Replacement	Calcite
700	Intermediate rock	Vesicle Replacement	Chlorite - Anhydrite - Calcite Calcite - Quartz
851	Intermediate rock	Fracture Replacement	Calcite Albite - Epidote
1001	Intermediate rock	Vesicle Vein	Epidote - Chlorite Quartz
1151	Intermediate rock	Vesicles	Chlorite - Epidote Chlorite - Epidote - Calcite Fine-grained clay - Anhydrite - Calcite
1302	Intermediate rock	Vesicle Replacement	Calcite - Epidote - Quartz Epidote - Quartz Albite - Epidote Albite - Calcite
1449	Intermediate rock	Replacement	Albite - Epidote - Actinolite Albite - Calcite
1900	Basalt	Vein Replacement	Epidote Albite - Actinolite Epidote - Quartz
2050	Intermediate rock	Replacement Vesicle	Epidote - Wollastonite - Anhydrite Epidote - Chlorite - Quartz
2351	Acidic rock	Replacement	Albite - Actinolite - Anhydrite

Table 3: Sequence of mineral deposition in well Fiale 3

5.3 Thermal history

To establish the thermal history of Fiale 3, a comparison of alteration minerals and measured temperatures has been undertaken to determine the current reservoir conditions in the area cut by the geothermal well. In the present study, the hydrothermal alteration temperature curve was obtained from the first occurrence of the minerals and their temperature of equilibrium needed for their formation. The minerals used are smectite ($\geq 40^\circ\text{C}$), quartz ($\geq 180^\circ\text{C}$), chlorite ($\geq 220^\circ\text{C}$), epidote ($\geq 230^\circ\text{C}$), and actinolite ($\geq 280^\circ\text{C}$). Measured temperatures and pressure were acquired from Turk et al. (2019) and Carver et al. (2019). The logs are presented in Figure 12.

The temperature logs were taken approximately two months after completion of the well, on 14th April 2019, and are compared to the alteration mineral temperatures. From the upper part to 390 m of the temperature log of 14th April 2019, the current temperature shows a slight cooling before reaching 214°C at 625 m (MD). This indicates a slight heating up compared to the quartz temperature (180°C). However, below this depth, high temperature minerals, e.g. epidote ($\geq 230^\circ\text{C}$) and actinolite ($\geq 280^\circ\text{C}$), occur at measured temperatures of 150°C and 74°C , respectively. It reflects a significant cooling of the reservoir between 733 m and 1700 m (MD). However, no mineralogical indications of the cooling are observed.

In the lower part of the well, the current temperature increases progressively and follows approximately the boiling point curve (BPC) from 2500 m and 2625 m. A maximum temperature of 362°C was recorded at 2625 m (MD).

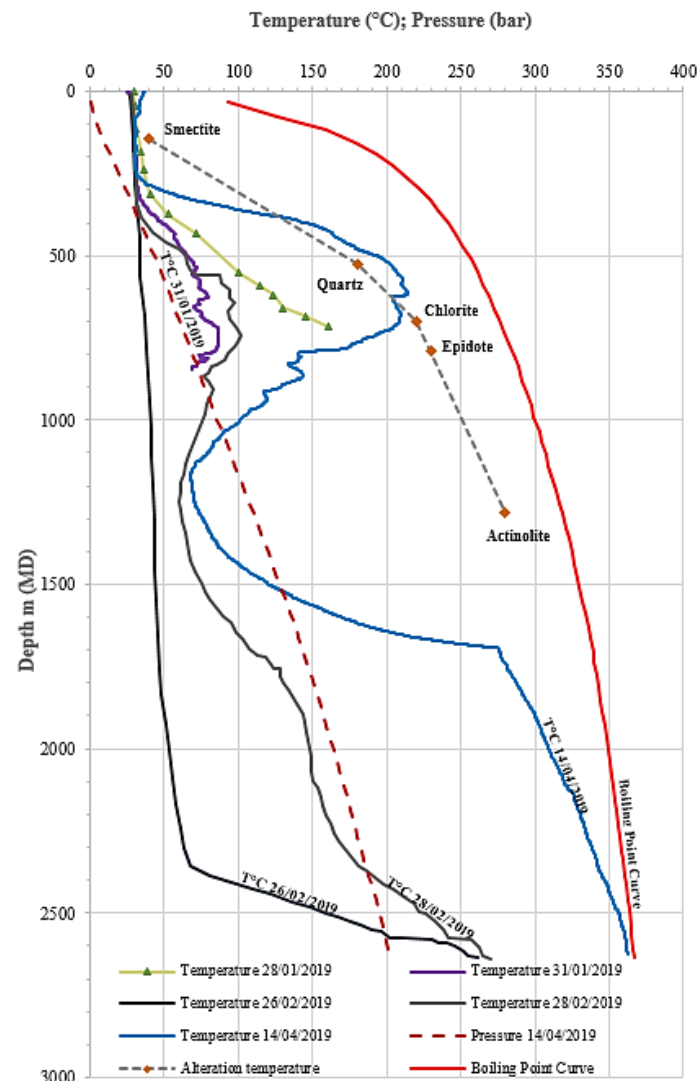


Figure 12: Temperature, alteration minerals, pressure and boiling point curve profiles of Fiale 3 (Turk et al., 2019; Carver et al., 2019).

5.4 Permeability zones

Feed zones are described as permeable layers able to produce significant amount of water. Aquifers refer to a geological formation, which can store and transmit water. The type of rock, permeability and the porosity are parameters that influence the flow of fluids. Two type of porosity exist. The primary one is formed during genesis of the rock such as the voids and pores. The secondary porosity appears after the rock was formed, and is produced by faults, joints, veins, or formation contacts (Reyes, 2000). Several parameters, which are circulation losses and/or gains, temperature and pressure logs, rate of penetration, alteration rate, are used as tools to identify permeable zones and aquifers/feed points in geothermal wells.

In well Fiale 3, the permeable zones are deduced mainly from circulation losses, temperature logs, alteration intensity based on the minerals indicative of permeability such as calcite or pyrite, and the results of the injection tests (Carver et al., 2019). The feed zones are described below and summarized in the Table 4.

During drilling, total losses of circulation occurred between 25 and 140 m, 180 and 185 m, 566 and 569 m, and 1736 and 1749 m depth. Temperature logs were obtained during and after drilling of the well. The results are presented by Carver et al. (2019). The temperature curves, in Figure 12, show minor feed points at 633 m, 817 m, 858 m and 933m. They demonstrate small decrease of the temperatures probably due to the intrusion of cold water. The largest inflow of cold seawater is at 733 m and results to a large reversal of temperatures up to 1700 m. This interval depth presents a high permeability rate controlled by the major faults NW-SE. Based on the alteration intensity observed during cutting analysis, this zone is associated to a high presence of calcite and pyrite in vein fillings. Two small feed zones are found at 2350 m and 2580 m depth. Spinner data (Carver et al., 2019) indicate fluid losses at the same depths, and at 2100 m.

Two injection tests have been carried out to test the permeability of the shallow reservoir between 500 and 850 m (Carver et al., 2019). The injectivity index (I.I.) is 0.97 kg/s/bar. It indicates a low permeability. Finally, the last injection test was conducted on 26th and 27th February 2019 to estimate the permeability of the deep reservoir between 1730 and 2660 m that corresponds to the interval depth of the slotted liner. According to Carver et al. (2019), the injectivity index shows a low permeability with 0.50 kg/s/bar.

Depth m (MD)	Rock type	Size	Remarks
25 - 140	-	Small	Total loss of circulation
180 - 185	-	Small	Total loss of circulation
566 - 569	-	Small	Total loss of circulation
633	Basalt	Small	Fracture/vein, small cold inflow
733	Intermediate rock	Large	Faults with large intrusion of cold seawater, abundance of calcite and pyrite
817	Intermediate rock	Small	Fracture/vein, small cold inflow, abundance of calcite and pyrite
858	Intermediate rock	Small	Fracture/vein, small cold inflow, abundance of calcite and pyrite
933	Intermediate rock	Small	Fracture/vein, small cold inflow, abundance of calcite and pyrite
1700	Intermediate rock	Small	Fracture, small increase of temperature
1736 - 1749	-	Small	Total loss of circulation
2100	Intermediate rock	Small	Fluid losses, small inflow of hot water
2350	Acidic rock	Small	Fluid losses, small inflow of hot water
2580	Acidic rock	Small	Fluid losses, small inflow of hot water
2600	Acidic rock	Small	small inflow of hot water
2650	Acidic rock	Small	small inflow of hot water

Table 4: Permeability zones identified in the well Fiale 3.

5.5 Correlation of Fiale wells and Asal 5

A stratigraphic correlation between wells Asal 5, Fiale 1, Fiale 2 and Fiale 3 was prepared by using Petrel software. The correlation results are mainly based on the stratigraphy of Asal 5, which is the most studied and described well in Fiale caldera area (Aqater, 1989).

Five stratigraphic units are found as shown in Figure 13. The upper part is formed by the recent volcanic unit of the Asal series. This unit consists dominantly of basalts. Then, the Afar stratoid series consist of basic and intermediate products. A thin layer of sedimentary unit deposited during Pliocene is found only in well Asal 5 and probably in Fiale 1. This layer marks the transition with the Dalha basalt unit. The Mabla rhyolite unit has been described in the Fiale wells based on cuttings analysis.

Occurrence of hydrothermal alteration minerals in several wells can help to analyze changes in the reservoir. To observe the distribution of alteration minerals and consequently the evolution of the reservoir in the four wells of Asal-Fiale geothermal field, a simple alteration model along a SW-NE cross-section was created with the Petrel software (Figure 14). Based on their equilibrium temperatures, smectite ($\geq 40^\circ\text{C}$), quartz ($\geq 180^\circ\text{C}$), chlorite ($\geq 220^\circ\text{C}$), epidote ($\geq 230^\circ\text{C}$), and actinolite ($\geq 280^\circ\text{C}$) have been chosen to establish the alteration zones. Moreover, current isotherms respectively of 40°C , 180°C , 220°C , 230°C and 280°C have been added to observe the actual thermal state of the geothermal reservoir. Fiale 1, Fiale 2 and Fiale 3 are deviated wells and Asal 5 is the only vertical well located outside the caldera. The wells are approximatively at the same level.

The results as illustrated by the model (Fig. 14), showing that the quartz zone is uniform except for Fiale 1 and 3 caused by thicker smectite zone and slight up-doming of the chlorite zone below. The epidote zone appears at slightly higher depth in the south-western part around Asal 5 and at deeper depth around Fiale 2 before rising slightly at Fiale 1. The actinolite isograd is found shallower at Asal 5 and Fiale 3 before rapidly going down at Fiale 2 and Fiale 1. This indicates that the temperatures were higher near Fiale 3 but without an emphasis of upflow zone.

Comparing to the isotherms obtained from measured temperatures in the wells, it shows a significant drop of the high temperatures. Indeed, 220°C , 230°C and 280°C isotherms are found at deeper depths below the actinolite isograd. This cooling is due to the large intrusion of cold seawater in the system throughout the major rift faults. Even though, no evidence for an upflow zone is noticed. This could indicate that the Fiale caldera is not an upflow zone at its current state, but rather shows characteristic patterns of an outflow zone.

6. DISCUSSION

Based on cutting analysis, the lithology of the well Fiale 3 consists mainly of fine- to medium-grained basaltic lava flows in the upper part of the well. Fine-to medium-grained intermediate rocks are found in the middle part, intercalated with some basaltic rocks. The bottom is mainly formed by fine-to medium-grained acidic rocks. According to the stratigraphic correlation between the wells, four main stratigraphic units are found, which are the Asal series, the Afar stratoid series, the Dalha basalt series and the Mabla rhyolite.

Petrographic studies allow to observe hydrothermal alteration minerals and define their paragenetic sequences. Alteration minerals are mainly found as replacements of primary minerals and in assemblage. They also have been observed as product of filling in vesicles, veins, and rare fractures. They include calcite and pyrite, which are used as indicators of permeability and are present in high amounts between 450 and 1250 m (MD). High-temperature minerals occur deeper. Epidote appears at 792 m, actinolite at 1283

m and wollastonite at 1371 m. The distribution of hydrothermal alteration minerals indicates a prograde evolution of the temperatures in the well. However, anhydrite, which is a sulphate rich mineral, is identified from 700 m onwards, indicating that seawater has been heated up and led to the precipitation of the mineral.

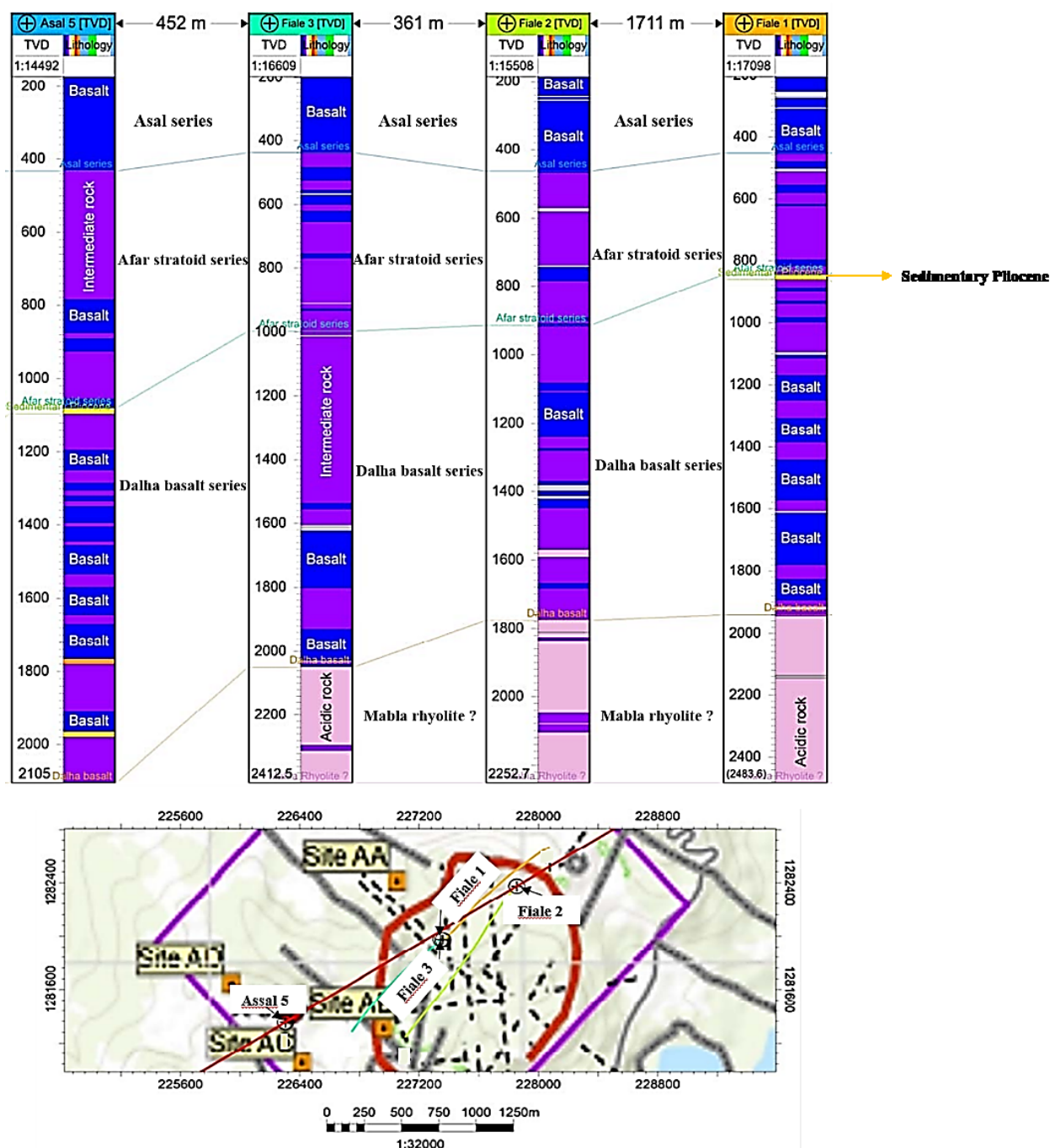


Figure 13: Stratigraphic correlation based on NE-SW cross-section between wells Asal 5, Fiale 1, Fiale 2 and Fiale 3. The lower image shows the location of the profile.

By compiling binocular, thin sections, methylene blue and XRD analyses, five alteration zones were recognized. In order of increasing depth, they are the smectite zone (145-550 m), chlorite zone (550-792 m), epidote zone (792-1283 m) and the epidote-actinolite zone (1283-2660 m). The unaltered zone is located in the upper part between the surface and 145 m (MD).

The occurrence of alteration minerals helped to establish the paleo-temperature curve. This latter is compared to the measured temperatures and boiling point curves. It shows a significant temperature reversal between 733 and 1700 m caused by a large inflow of cold seawater, as shown in Figure 12. Moreover, this cooling is shown by the presence of anhydrite rarely in sequences (Table 3). It is also important to note that the cold zone does not present other low-temperature minerals. Below 1250 m, the temperature starts to increase progressively and follows the boiling point curve (BPC) in the lowest depths. A maximum temperature of 362°C was recorded at 2625 m (MD). Therefore, the discrepancies between the alteration minerals and current temperatures indicate that Fiale 3 is not in state of equilibrium. Furthermore, the absence of lower temperature minerals in the cold zone could demonstrate that the inflow of cold seawater may be geologically young.

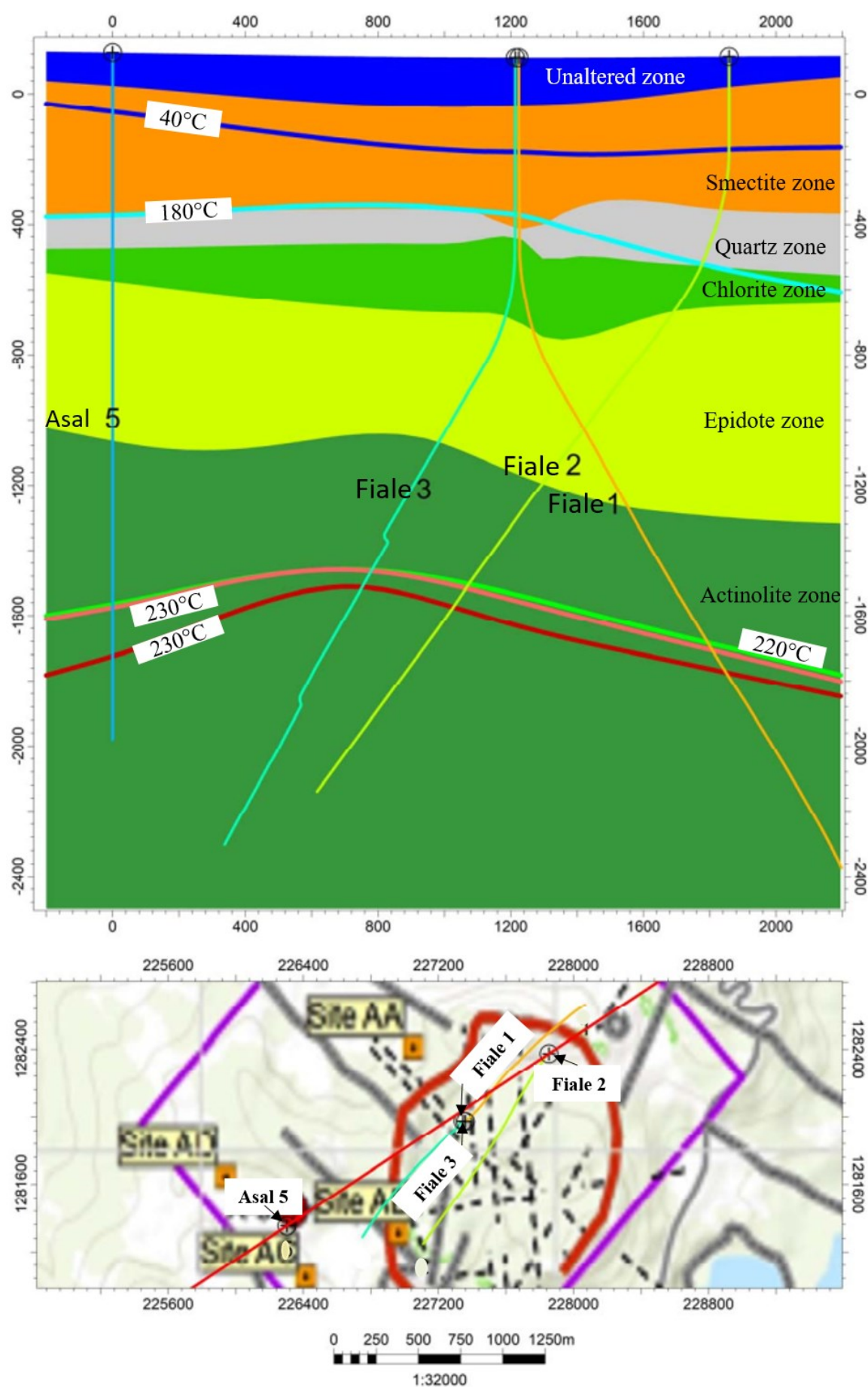


Figure 14: Alteration model (upper image) based on cross-section in SW-NE between wells Asal 5, Fiale 1, Fiale 2 and Fiale 3. The lower image shows the location of the profile.

By analyzing the measured temperature curves and reservoir testing results, feed zones are mainly associated to circulation losses in the shallow part of the well. The temperature profiles show also minor feed points at 633 m, 817 m, 858 m and 933 m indicating small cooling. The largest feed point is noted at 733 m (MD) causing the temperature reversal of Fiale 3. The cold inflow is explained by the infiltration of seawater from the Ghoubbet bay to the Asal Lake through the major trend NW-SE faults. Three more small feed points during the increasing of temperatures are found at 1741 m, 2100 m, 2350 m, and 2580 m. The injection tests show the existence of a shallow reservoir relatively hot between 500 and 850 m (MD). It presents a low permeability also found in the lower part of the well.

A simple alteration model has been created with the help of Petrel software. The model shows that the alteration zones are approximately uniform through the Fiale caldera, except that small up-doming of the chlorite, epidote and actinolite isograds are observed at well Fiale 3. It indicates that the temperatures were higher in this zone but without any evidence of hot up-flow zone. By comparing the current isotherms to the alteration isograds, it shows a significant cooling of the reservoir. The isotherms of 220°C, 230°C and 280°C, are observed below the actinolite isograd. The cooling of the reservoir is caused by the large inflow of cold seawater from Ghoubbet bay toward the Asal Lake through the NW-SE faults of the rift. A small up-doming of the isotherms is noticed near Fiale 3 at greater depths but without any emphasis of up-flow zone. It could indicate that the Fiale wells and Assal 5 are situated in an outflow zone.

7. CONCLUSION

The study of the well Fiale 3 has provided a first comprehensive overview of the lithology, alteration mineralogy, thermal history and permeability within the Fiale caldera. Based on the obtained results, the following can be concluded:

- The lithostratigraphy of Fiale 3 is divided into four stratigraphic units which are the Afar series in the upper part, the Afar stratoid series, Dalha basalt series and the Mabla rhyolite in the bottom of the well. However, the stratigraphic correlation is based on cuttings analysis and comparison with Asal 5 well. Further analyses are needed to confirm the lithostratigraphic distribution in Fiale 3, in particular the chemical nature of the stratigraphic units.
- Hydrothermal alteration minerals in well Fiale 3 are found as product of replacement of primary minerals and fillings in vesicles, veins and fractures. High temperature minerals such as albite, epidote, actinolite, and wollastonite are described. Anhydrite is also noted from 700 m onwards, which is an indicator of seawater intrusion.
- In total, five alteration mineral zones are identified. They are: unaltered zone (<145 m), smectite zone (145-550 m), chlorite zone (550-792 m), epidote zone (792-1283 m) and epidote-actinolite zone (1283-2660 m).
- Thermal history of Fiale 3 demonstrates a shallow cooling of the geothermal system due to the large intrusion of cold seawater throughout the NW-SE major faults of the Asal-Ghoubbet rift. Anhydrite is an indicator of the cooling in regards of alteration mineralogy. However, low-temperature minerals are not observed by any applied method. The differences between alteration and measured temperatures may correspond to a recent cooling and high-temperature minerals are relicts of former geothermal system with higher temperatures. However, it seems to be clear that the well is heating at its deepest part. Further analysis such as fluid inclusion analysis could help to better describe the impact of the reversal temperature within the geothermal system.
- The injection tests describe two reservoirs. A shallow reservoir between 500 and 850 m with a maximum temperature of 214°C and low permeability. The second reservoir between 1783 and 2660 m also indicate a low permeability. The largest feed zone corresponds to the inflow of seawater at 733 m. In general, it seems that the well has a low permeability.
- Finally, the correlation of hydrothermal alteration zones and currents isotherms between Fiale wells and Assal 5 located outside the caldera, show that the area is located in an outflow zone with no indication for an active upflow zone. Moreover, the model also demonstrates the cooling of the geothermal system caused by the intrusion of cold seawater through the major faults of the Assal-Ghoubbet rift. Further geothermal exploration is needed to locate the possible up-flow zone in the area.

REFERENCES

- Abdallah, A., V. Courtillot, M. Kasser, A. Y. Le Dain, J.-C. Le'pine, B. Robineau, J.-C. Ruegg, P. Tapponnier, and A. Tarantola, 1979: Relevance of Afar seismicity and volcanism to the mechanics of accreting plate boundaries, *Nature*, 282, 17–23.
- AfDB, 2013: Geothermal exploration project in the Lake Assal region. African Development Bank, Rabat, 31 pp.
- Ahmed, M., 2008: Borehole geology and hydrothermal mineralization of well HN-08, Hellisheidi geothermal field, SW-Iceland. Report 8 in: Geothermal training in Iceland 2008. UNU-GTP, Iceland 1-29.
- Aquater, 1989: Djibouti geothermal exploration project. Republic of Djibouti. Aquater S.p.a report A3770. 159 pp.
- Árnason, K., Björnsson, G., Flóvenz, Ó. G. and Haraldsson, E. H., 1988: Geothermal Resistivity Survey in the Assal Rift in Djibouti. Volume I: Main text. OS-88031/JHD-05. 49 pp.
- Árnason, K., Eysteinnsson, H. and Vilhjálmsón, A. M., 2008: The Assal geothermal field, Djibouti. Geophysical surface exploration 2007–2008. Iceland GeoSurvey, ÍSOR-2008/019. 77 pp.
- Audin, L., Manighetti, I., Tapponnier, P., Me'tivier, F., Jacques, E., and Huchon, P., 2001: Fault propagation and climatic control of sedimentation on the Ghoubbet Rift Floor: Insights from the Tadjouraden cruise in the western Gulf of Aden, *Geophys. J. Int.*, 144, 391–413.

- Barberi, F., Ferrara, G., Santacroce, R., Varet, J., 1975: Structural evolution of the Afar triple junction. In: Pilger, A., Rösler, A. (Eds.), *Afar Depression of Ethiopia*, vol. 1. Schweizerbart, Stuttgart, Germany, pp. 38–54.
- Bird, D.K., Schiffman, P., Elders, W.A., Williams, A.E., and McDowell, S.D., 1984: Calc-silicate mineralization in active geothermal systems. *Economic Geology*, 79, 671–695.
- BRGM, 1973: Geophysical study using Melos surveys and electric surveys in the Lake Asal region (TFAI). BRGM office, Orléans, France, report (in French), 18 pp.
- Browne, P.R.L., 1978: Hydrothermal alteration in active geothermal systems. *Ann. Rev. Earth Planet. Sci.*, 6, 229–250.
- Carver, C. T., Garg, S. K., Davis, L.C., and Jalludin, M., 2019: Reservoir characterization from exploration well completion tests in the Fiale caldera, Djibouti. *Proceedings of GRC Transaction*, Vol. 43, 14 pp.
- Courtillot, V., Armijo, R., and Tapponnier, P., 1987: Kinematics of the Sinaium; Triple Junction and a two-phase model of Arabia-Africa rifting, in *Continental Extensional Tectonics*, edited by M. P. Coward, J. F. Dewey, and P. L. Hancock, *Geol. Soc. Spec. Publ.*, 28, 559–573.
- Courtillot, V., Jaupart, C., Manighetti, I., Tapponnier, P. and Besse, J., 1999: On causal links between flood basalts and continental breakup, *Earth Planet. Sci. Lett.*, 166, 177–195.
- De Chabaliér, J.-B., and Avouac, J.-P., 1994: Kinematics of the Asal Rift (Djibouti) determined from the deformation of Fiale Volcano, *Science*, 265, 1677–1681.
- Demange, J. and Puvilland, P., 1990 : *Champ géothermique d'Assal, Djibouti; synthèse des données*, BRGM.
- Demange, J., Stieltjes, L., and Varet, J., 1980: L'éruption d'Assal de Novembre 1978, *Bull. Soc. Geol. Fr.*, 7, 837–843.
- Dobre, C., Manighetti, I., Dorbath, C., Dorbath, L., Jacques, E., & Delmond, J., 2007: Crustal structure and magmato-tectonic processes in an active rift (Assal-Ghoubbet, Afar, East Africa): 1. Insights from a 5-month seismological experiment. *JOURNAL OF GEOPHYSICAL RESEARCH*, VOL. 112.
- Henley, R. W. and Ellis, A.J., 1983: Geothermal systems ancient and modern: a geochemical review. *Earth Science and Reviews*, 19, 1–50.
- ISERST, 1985: Carte géologique de la République de Djibouti à 1:100,000: Tadjoura. République de Djibouti.
- ISERST, 1986: Carte géologique de la République de Djibouti à 1:100,000: Ali Sabih. République de Djibouti.
- Khodayar, M., 2008: Results of the 2007 surface geothermal exploration in the Assal Rift and Transform zones, Djibouti. *Tectonics and Geothermal manifestations*. Iceland GeoSurvey, ÍSOR-2008/008. 70 pp + annex + 5 maps.
- Kristmannsdóttir, H., 1976: Type of clay minerals in hydrothermally altered basaltic rocks. *Jökull*. 26, 30–39.
- Kristmannsdóttir, H., and Tómasson, J., 1978: Zeolite zones in geothermal areas in Iceland. In: Sand, L.B., and Mumpton (eds.), *Natural zeolites, occurrence, properties, use*. Pergamon Press Ltd., 277–284.
- Le Gall, B., Daoud, A. M., Maury, R., Gasse, F., Rolet, J., Jalludin, M., and Moussa, N., 2015: *Geological Map of the Republic of Djibouti*. Djibouti: CERD.
- Manighetti, I., King, G. C. P., Gaudemer, Y., Scholtz, C. H., and Dobre, C., 2001a: Slip accumulation and lateral propagation of active normal faults in Afar, *J. Geophys. Res.*, 106, 13,667–13,696.
- Manighetti, I., Tapponnier, P., Courtillot, V., Gallet, Y., Jacques, E. and Gillot, Y., 2001b: Strain transfer between disconnected, propagating rifts in Afar, *J. Geophys. Res.*, 106, 13,613–13,665.
- Manighetti, I., Tapponnier, P., Gillot, P.-Y., Jacques, E., Courtillot, V., Armijo, R., Ruegg, J.-C., and King, G., 1998: Propagation of rifting along the Arabia-Somalia plate boundary: Into Afar, *J. Geophys. Res.*, 103, 4947–4974.
- Marks, N., Schiffman, P., Zierenberg, R.A., Franzson, H., and Fridleifsson, G.Ó., 2010: Hydrothermal alteration in the Reykjanes geothermal system: Insights from Iceland deep drilling program well RN- 17. *J. Volcanol. & Geothermal Research*, 189, 172–190.
- Moore, D.M., and Reynolds Jr., R.C., 1989: *X-ray diffraction and identification and analysis of clay minerals* (18th ed.). Oxford University Press, Oxford, 378 pp.
- Ngoc, P. V., Boyer, D., Mouel, J. L. and Courtillot, V., 1981: Identification of a Magma Chamber in the Ghoubbet-Assal Rift (Djibouti) from a Magnetotelluric Experiment. *Earth and Planetary Science Letters* 52, 372–382.
- Pinzuti, P., 2006 : *Croissance et propagation des failles normales du rift d'Assal-Ghoubbet par datations cosmogéniques ³⁶Cl-Liens avec le magmatisme*, Ph.D. Thesis, IPGP, France.

- Reyes, A.G., 2000: Petrology and mineral alteration in hydrothermal systems: from diagenesis to volcanic catastrophes. UNU-GTP, Iceland, report 18-1998, 77 pp.
- Ruegg, J.-C., Le'pine, J.-C., and Tarantola, A., 1979: Geodetic measurements of rifting associated with a seismo-volcanic crisis in Afar, *Geophys. Res. Lett.*, 6, 817–820.
- Spürgin S., Weisenberger T.B., and Marković M., 2019: Zeolite-1 group minerals in phonolite-hosted deposits of the Kaiserstuhl Volcanic Complex, Germany, *Am. Min.*, 104, 659-670.
- Stefánsson, A., Gíslason, S.R. and Arnórsson, S., 2001: Dissolution of primary minerals in natural waters. II. Mineral saturation state. *Chemical Geology*, 172, 251-276.
- Stein, R., Briole, P., Ruegg, J.-C., Tapponnier, P., and Gasse, F., 1991: Contemporary, Holocene, and Quaternary deformation of the Asal Rift, Djibouti: Implications for the mechanics of slow spreading ridges, *J. Geophys. Res.*, 96, 21,789–21,806.
- Tapponnier, P., Armijo, R., Manighetti, I., and Courtillot, V., 1990: Bookshelf faulting and horizontal block rotations between overlapping rift zones in southern Afar, *Geophys. Res. Lett.*, 17, 1–4.
- Tarantola, A., Ruegg, J.-C., and Lépine, J.-C., 1979: Geodetic evidence for rifting in Afar: A brittle-elastic model of the behaviour of the lithosphere, *Earth Planet. Sci. Lett.*, 45, 435– 444.
- Tarantola, A., Ruegg, J.-C., and Lépine, J.-P., 1980: Geodetic evidence for rifting in Afar, 2. Vertical displacements, *Earth Planet. Sci. Lett.*, 48, 363–370.
- Turk, J., Haizlip, J., Mohamed, J., Mann, M., Letvin, A., and Moussa, N., 2019: A comparison of alteration mineralogy and measured temperatures from three exploration wells in the Fiale caldera, Djibouti. *Proceedings of GRC Transaction*, Vol. 43, 11 pp.
- Varet, J., 1978: Geology of central and southern Afar (Ethiopia and Djibouti Republic), *Centre Natl. de la Res. Sci.*, Paris, 124 p.
- Verhoef, P.N.W., 1992: The methylene blue adsorption test applied to geomaterials, *Memoirs of the Centre of Engineering Geology in the Netherlands, Delft University of Technology*, No.101, GEOMAT.02, 70 p.
- Weisenberger T., and Selbekk R.S., 2009: Multi-stage zeolite facies mineralization in the Hvalfjörður area, Iceland, *Int. J. Earth Sci.*, 98, 985-999.